Estimation of the exposure of buildings to driving rain in Spain from daily wind and rain data

José M. Pérez-Bella[a], Javier Domínguez-Hernández[a*], Beatriz Rodríguez-Soria[a], Juan J. del Coz-Díaz[b], Enrique Cano-Suñén[a]

[a] *Department of Construction Engineering, Engineering and Architecture School, University of Zaragoza (UZ), María de Luna, s/n, 50018, Zaragoza, Spain*

[b] *Department of Construction Engineering, University of Oviedo, Edificio Departamental Viesques nº 7, 33204 Gijón, Spain.*

Abstract

In this study, the severity of the exposure of buildings in Spain to driving rain is estimated. The annual driving rain index (*aDRI*) is determined at 80 sites spread across Spain, based on wind and rain data recorded daily over 30 years. The comparison among the driving rain indices based on daily, monthly and annual climatic data, allows assessing the existence of co-occurrence errors and errors due to averaging. This work also introduces a new reference scalar index to characterise exposure to driving rain during the wetting stages of the building façades based on daily data. Therefore, a new approach to the concept of "spell" established by the ISO 15927-3:2009 standard is proposed. The combination of the two indices provides a qualitative characterisation based on two temporal criteria, supplementing the estimated exposure level currently set by the Spanish standard for the design of buildings. A driving rain map for Spain is produced. Those sites where exposure during periods of wetting is significant are identified (the northern part of the country, the Gulf of Cadiz and specific areas of the Mediterranean coast and the Canary Islands). An important annual exposure on the north and northwest coast of the country and a slightly lower exposure in coastal areas of the Gulf of Cadiz are also identified. The Mediterranean coast and the interior regions are considered to have a low annual exposure to driving rain. Finally, the major findings of this research are reported.

Keywords

Driving rain, Wind speed, Rainfall, Building design, Spain

[*] Corresponding author. Department of Construction Engineering, University of Zaragoza (UZ), María de Luna, s/n, 50018, Zaragoza, Spain. Tel.Fax: +34 976 76 21 00.
E-mail address: javdom@unizar.es (Javier Domínguez-Hernández)

1. Introduction

Atmospheric precipitation accompanied by gusts of wind is primarily responsible for the wetting of and penetration of water into building façades. Moisture in the building façades causes a large amount of damage, a decrease in façade durability and an increase in maintenance costs [1-2]. The moisture also affects the hygrothermal behaviour of the building façades, reducing insulation performance and energy savings [3-5].

Due to its Atlantic-Mediterranean location and its strong topography, Spain experiences pronounced climatic variations, ranging from steppe and desert areas (southeast of the Iberian Peninsula and Canary Islands) to climates without a dry season (in the northern Iberian Peninsula), resulting in very different exposure to driving rain.

Climatic records of rain and wind in each region enable the estimation of the characteristic exposure of each site to driving rain. This estimation is an essential prerequisite for the implementation of building regulations and methodologies of performance-based design that are intended to prevent syndromes related to moisture.

In Spain, an estimation of the driving rain exposure when designing façades has been required since 2006, when the Technical Building Code (SBTC) [6] was published. Prior to this date, this estimation was not considered necessary. However, the estimation provided by the standard requires profound improvements, and the results are not currently comparable with those obtained using the methodologies established in other countries.

This article examines the climatic data recorded by 80 meteorological stations located at airports in major Spanish cities and towns, representing the entire Spanish mainland and its Balearic and Canarian archipelagos. From this analysis, we estimated an annual index (*aDRI*) to characterise the exposure to driving rain associated with the site that is comparable to the estimations established in other countries.

Additionally, the exposure during specific stages of wetting associated with the site was approximated by defining a new index, I_{AS}.

2. Background

The simultaneous measurement of rain and wind during atmospheric precipitation allows the characterisation of the amount of rain diverted by the wind onto a vertical surface. During the 1950s and 1960s, Hoppestad [7] and Lacy [8] addressed the study of the relationship between rain and wind and driving rain on vertical surfaces. The methodologies and indicators that currently allow the semi-empirical estimation of exposure to driving rain on façades and vertical building envelopes are based on this work. A general review of the state-of-the-art of wind-driven rain (WDR) research was provided by Blocken and Carmeliet [9]. Comprehensive comparative analysis of these semi-empirical methodologies has also been recently presented [10]. In spite that other estimation methods based on CFD can provide more accurate and less limited results than the semi-empirical methods [11-12], the latter are easy to use and allow to obtain initial estimations of overall exposure at different locations.

These semi-empirical methods are based on theoretical formulations and coefficients adjusted (at least partly) from measurements. To determine the driving rain on building façades, the "free-field" exposure calculated must be multiplied by some correction factors, dependent on the surroundings and characteristics of the analyzed building. Since this work estimates airfield exposure indices (at a height at 10 meters above ground level in the middle of an airfield or open field, at the geographical location of the wall), these correction factors are not applied.

The accuracy of these airfield indicators of exposure varies depending on (among others) the consideration of the wind direction and the accuracy of the available climate data (the recording

frequency of the information) [13-14]. In this context, two types of procedures (scalar and directional) can be defined to characterise exposure to driving rain.

Scalar indices allow for a global characterisation of the exposure linked to each location without identifying the specific orientation at which the exposure is most pronounced. The indices are of great simplicity and can be calculated from basic data for wind and rain that are available. This simplicity allowed Lacy and Shellard [15], in 1962, to propose the driving rain index (*DRI*) as a standard to characterise the scalar exposure linked to each site.

This index is usually computed annually as *aDRI* and represents the product of the rainfall and the average wind speed simultaneous, qualitatively characterising the moisture exposure over time. The ready availability of the data required for this calculation has led to this index being studied in many countries, such as the UK, Norway, the USA, Canada, Greece, Turkey, China and India, among others [16-21], which allows for an international comparison of exposure levels. This paper analyses the Spanish case, allowing for the comparison of its rates of exposure with those of other countries.

Directional indices (based on the "cosine projection method"), also need the wind direction simultaneously with rainfall data to estimate the orientation from which the driving rain is approaching. The results obtained predict the amount of driving rain expected for each orientation and thus generate an independent exposure for each possible direction [22]. The ISO 15927-3:2009 [23] established a procedure for the quantitative estimation of various directional indicators of exposure, both on an annual basis (I_A) and per spell (I_S). To ensure the accuracy of the method, climate data must be recorded at very short intervals, generally by the hour [24].

However, the simultaneous hourly data for rainfall, wind speed and wind direction required for this directional calculation are often unavailable in many countries (the data do not cover enough years and are therefore insufficient, or the number of sites is not very representative). Thus, the directional

calculation is typically restricted to specific points where there are stations with adequate availability of these data [25].

In Spain, automatic weather stations that are fully capable of measuring real-time weather conditions began to be installed in the late 1990s; therefore, there are no hourly data old enough to enable a representative study at a significant number of sites.

Due to these difficulties, several methods of approximation of the directional indicators based on more accessible climate data have been developed. Examples include the alternative method also recommended by the ISO, which uses average wind data and synoptic records for rain, and the method proposed by Rydock [26] that has been applied in different cities in Norway, which also utilises synoptic meteorological records. This article defines an alternative scalar approximation, based on daily weather data for rain and wind, from the definition of the directional index I_S used by the semi-empirical ISO model.

The definition of this scalar indicator (I_{AS}), referring to short periods of time, provides an estimate that complements the annual characterisation of the *aDRI* index. Whereas annual exposure characterises the moisture content of the façades in the long term, the exposure during stages of wetting determines the instantaneous risk of water penetration through the façades.

2.1 Spanish background

Despite the momentum imparted by the meeting of the CIB (International Council for Research and Innovation in Building and Construction) Working Commission on Rain Penetration in Madrid in 1966 [27], which presented elaborated *aDRI* values for different countries, driving rain has been overlooked as a relevant parameter for the design of the façades on Spanish buildings. Only after the SBTC came into effect in 2006 did the demand for protection against moisture became crucial in façade design [6].

The Spanish standard defines five different degrees of exposure to moisture, the determination of which is based on maps of wind and rainfall (Figure 1). The height of the building, the terrain roughness and the specific wind zone for the location constitute three possible ranges of exposure to wind (V1 to V3). The limits of these ranges are difficult to measure, due to the fact that numerical values are not associated with the parameters for the terrain roughness or building height (Table 1). Based on this exposure to wind and the annual rainfall in the area of the site (zones I to V), the degree of exposure to moisture in the building (Table 2) is determined, which will, in turn, be used to determine the façade construction solutions allowed in each case.

Fig. 1. Map of wind zones (A, B, C) for wind gusts of 10 minutes and a 50-year return period (left) and the map of average annual rainfall zones (right) used by the Spanish standard. Source: SBTC (DB-HS1).

Table 1. Determination of the degree of exposure to wind. Source: SBTC (DB-HS1).

Table 2. Determination of the degree of exposure to moisture. Source: SBTC (DB-HS1).

This characterisation is based on allocations by tables and zone maps and does not provide a numerical calculation, making it highly subjective and not very performance-based. Thus, it is not possible to estimate a specific value of driving rain associated with each degree of exposure or to establish precise comparisons of exposure between sites. In the same characterisation, certain local parameters are included, such as the building height or terrain roughness; however, others do not apply, such as the wall factor or topographic coefficient [23, 28].

Moreover, the climatic data for wind and rain used in the estimation are not simultaneous, nor do they belong to similar intervals of time. For the mapping of rainfall, the data used were the average annual rainfall measurements. For the elaboration of the wind map, maximum wind gusts were assessed at intervals of 10 minutes for a return period of 50 years. Thus, the starting maps are not correlated.

Because the method presented above does not assume principles similar to those used in other countries, it is not possible to objectively provide reviews and comparisons with other international arenas. Because the estimate is indirect, there is no map that uniquely characterises the exposure associated with each site. This article overcomes these shortcomings by characterising exposure based on the current state of the art and improving the estimate established by the Spanish standard. To accomplish this task, we analyse the daily weather data collected by the Spanish Meteorological Agency (AEMET) at 80 meteorological stations.

3. Computation of the annual driving rain index from daily data

Among the historical series of climatic data provided by AEMET [29], we have selected those that incorporate more than 30 years of data (80 stations). Of these, 35 stations have 50 years of weather records (1962-2011). These stations are scattered throughout Spain and are representative of different varieties of climate and topography.

The available data contain daily records of rainfall R_{hD} (mm) and mean wind speed U_{10D} (m/s), allowing for the calculation of the scalar indicator of annual exposure *aDRI* based on daily records (*daDRI*). The annual rate is expressed in m^2/s, by Eq. (1), where D is the total number of days included in the climatic data:

$$daDRI = \frac{\sum_{i=1}^{D} \frac{R_{hD}}{1000} \cdot U_{10D}}{number\ of\ considered\ years} \quad (1)$$

The indices calculated for each site (Table 3) enable their classification according to the ranking established by Lacy [15]: <3 m^2/s represents "sheltered exposure", 3-7 m^2/s represents "moderate exposure", 7-11 m^2/s represent "high exposure" and >11 m^2/s represents "severe exposure". The geographical distribution of the results obtained is shown in Figure 2.

Table 3. Driving rain indices for 80 sites spread across the Spanish territory *(stations with daily records for 50 years are italicised).*

From these results, it can be observed that 25% of the sites studied have a "non-sheltered" exposure, and the majority are concentrated along the north Atlantic coast (Santiago de Compostela, San Sebastián, Vigo, Santander) and the Gulf of Cadiz (Tarifa, Jerez, Cadiz).

Despite the distinct climates of these areas [30], the presence of Atlantic winds of greater intensity than in the rest of the country results in conditions of marked driving rain, which must be anticipated through the proper design of the building façades in these locations.

A wide variation in the indicator is identified, from negligible values of 0.6 m^2/s obtained in areas of desert or steppe climate (the coast of the Canary Islands, Murcia) to severe or high exposure values in locations of weather without a dry season (the Atlantic coast in the north and northwest of the country).

In inland areas and the Mediterranean coast, the exposure is generally sheltered, except at locations at high altitudes. It can be observed that the height of a station (above 1,500 m) can produce sharp variations of exposure in small geographic areas, such as in the mountain station of the island of Tenerife (Izaña)

and in the mountain pass of Navacerrada. Neither result is representative of normal conditions in urban areas, detracting from the other results. Therefore, these two stations were not used for the subsequent analysis.

Fig. 2. Annual Driving Rain Index Map of Spain.

3.1 Relationship between daDRI, maDRI and aaDRI

The accuracy in estimating driving rain directly depends on the frequency of collection of climate data. A shorter time between registers ensures a more accurate measure of the average wind speeds and, therefore, a more realistic indicator. The daily records available for the whole country have enabled the establishment of a first estimate of exposure that is of higher accuracy than that obtained if monthly or annual average data were used. This estimate is commonly applied in several studies in the absence of more detailed data [17] [19-21].

To expand the scope of this work, we have compared the *aDRI* index based on daily data (*daDRI*), with results based on monthly (*maDRI*) or annual (*aaDRI*) average data for wind and rain (Table 3). From the comparison of the results, it is possible to establish adjustments that allow for the extrapolation of accurate (daily) exposure estimates from average monthly or annual data. To this end, Figures 3 and 4 shows the best linear fit possible between the different indices for the 78 stations analysed (excluding the mountain stations).

These daily, monthly and annual data do not incorporate the simultaneity of wind and rain and so all the wind data recorded are averaged, even without rainfall. Nevertheless, daily data provide a better basis

than monthly or annual data for index calculation. The analysis has been performed for the same intervals of time that were considered for the *daDRI* index at each of the stations.

Fig. 3. Best-fit linear relationship between *daDRI* and *maDRI*.

Fig. 4. Best-fit linear relationship between *daDRI* and *aaDRI*.

Although the analysed stations are scattered throughout the Spanish territory, a high correlation coefficient (R^2) is identified. This observation validates the possibility of extrapolating the above adjustments to any other Spanish location. Based only on monthly or annual averages of rainfall and wind speed (values that are available for a large number of locations), the *daDRI* index, which exhibits greater precision than *aaDRI* or *maDRI*, could be estimated in this way for a much larger number of sites.

A similar relationship can be established between the monthly and annual results. The fit obtained, shown in Figure 5, is very similar to that obtained by other studies conducted in countries with Mediterranean climate, such as Greece [18]. Similarly, previous *daDRI* value adjustments could also be considered useful in improving the accuracy of the exposures calculated from monthly or annual data in locations with climates similar to that of Spain. By contrast, in places with very different climates [21], the adjustment identified between *maDRI* and *aaDRI* is very different (see figure 6).

Fig. 5. Best-fit linear relationship between *maDRI* and *aaDRI*.

Fig. 6. Comparison with Greek and Indian maDRI-aaDRI adjustments.

3.2 Data averaging and co-occurrence error

In a second analysis, we studied the relative influence of each of the possible sources of error inherent in the use of monthly and annual averages of wind and rain. These sources of error are due to omitting to consider the co-occurrence (e_1) of both phenomena and to the mathematical averaging of the data (e_2) [13].

To determine the magnitude of each error factor, the same previous calculation was performed, dismissing from the monthly and annual averages those daily wind records corresponding to days without precipitation. Because there is no averaging of wind values with non-simultaneous precipitation, this approach partly eliminates the error of co-occurrence, obtaining indices of exposure to driving rain with a significantly lower error rate.

The analysis of these indices in the 78 Spanish stations (N = 78) reveals the magnitude of the co-occurrence error (e_1), with an average deduction of 6.98% when using monthly mean data and 6.75% in the case of annual data. The complementary error (e_2) corresponds logically to the uncertainty provided by the same arithmetic averaging of the climate data in the monthly and annual ranges (Figures 7 and 8 represent the most exposed sites and table 4, all the sites).

$$\text{Monthly average } e_1 = \sum_{i=1}^{N} \frac{e_{1_i}}{daDRI_i} \cdot 100 \Big/ N = -6.98\% \tag{2}$$

$$\text{Annual average } e_1 = \sum_{i=1}^{N} \frac{e_{1_i}}{daDRI_i} \cdot 100 \Big/ N = -6.75\% \tag{3}$$

$$\text{Monthly average } e_2 = \sum_{i=1}^{N} \frac{e_{2_i}}{daDRI_i} \cdot 100 \Big/ N = -6.99\% \quad (4)$$

$$\text{Annual average } e_2 = \sum_{i=1}^{N} \frac{e_{2_i}}{daDRI_i} \cdot 100 \Big/ N = -7.06\% \quad (5)$$

Fig. 7. Exposure indices calculated from the monthly average data according to both hypotheses in non-sheltered annual exposure stations. (e_1) The magnitude of the error derived from the non-co-occurrence of wind and rain. (e_2) The magnitude of the error derived from the averaged data.

Fig. 8. Exposure indices calculated from the annual average data according to both hypotheses in non-sheltered annual exposure stations. (e_1) The magnitude of the error derived from the non-co-occurrence of wind and rain. (e_2) The magnitude of the error derived from the averaged data.

Table 4. Summary of the errors derived from the non co-occurrence of wind and rain (e_1) and from the averaged data (e_2) at 78 Spanish sites.

Compared to daDRI, the sum of both errors causes an average deduction in the exposure that is close to 13.9%, using monthly or annual average data. The adjustments identified in Figures 3 and 4, applied to any Spanish location, allow for a great reduction in these errors intrinsic to the estimation of the indices *maDRI* and *aaDRI*.

We conclude that, in the Spanish climate, the relative weights of both sources of error in estimating the annual index of exposure to driving rain are very similar. This error compensation also provides real data, not just theoretical, emphasising the importance of both sources of error and revealing the need for alternatives proposed by several authors to minimise the error due to monthly or annual averaging of climatic data [13].

4. Proposed method for the scalar estimation of the airfield spell index from daily data

Directional indices provide a more accurate estimate for driving rain since they consider wind directionality. In particular, the airfield index I_S is associated with spell, a concept established by the standard ISO 15927-3:2009 that provides an indication of exposure associated with specific time periods shorter than the annual interval [10].

This I_S (mm/spell) index is used to estimate the probability of driving rain penetration through heavy façades (masonry) during time intervals in which the supply of water due to rain is greater than the loss due to evaporation. This time interval (spell) is defined by the ISO standard as being limited by the occurrence of at least 96 hours devoid of driving rain from a specific orientation, i.e. a different spell is defined over each orientation.

Considering the driving rain during each of the spells in one year I'_S, it is possible to obtain a reference value, I_S, associated with the maximum expected value in a 3-year interval. Each possible orientation of the façade has a corresponding exposure and thus a differential value.

The estimate of driving rain during each spell I'_S is obtained by using hourly records of rainfall R_h (mm), wind U_{10} (m/s) and wind direction D (º) in relation to an orientation Θ (º), opposite in direction to the outer perpendicular of the façade. In the summation, only the positive results, i.e., only those hours when the wind drives a certain amount of rain onto the façades, are considered (see Eq. (6))

$$I'_S = \frac{2}{9}\sum U_{10} \cdot \left(R_h\right)^{8/9} \cdot \cos\left(D - \Theta\right) \quad (6)$$

4.1 Scalar approach to the airfield spell index

Heavy masonry façades are predominant in Spain. Between the years 2007-2010, 48.8% of new buildings had masonry coatings, and if masonry coated with stucco and plaster mortar is also considered, 80.7% of new buildings had masonry coatings [31]. It is therefore particularly important to define performance-based designs adapted to the climate [32].

For this task, the estimation of exposure periods related to spells (I_S) is also necessary. However, the hourly data are not sufficient, nor are there daily data related to wind direction. To overcome this problem, we define a scalar approach to the concept of driving rain during wetting stages (I_{AS}), using the above daily data series.

A new concept called "Absolute Spell", which is limited by the occurrence of four days (96 hours) devoid of driving rain at the site, was defined. When omitting the orientation of the façades, any precipitation produced helps to prolong the period, regardless of wind direction. Therefore, the duration of the period is always slightly higher than that calculated according to the ISO standard.

Fig. 9. Definition of "ISO spell" and proposed "absolute spell".

Using the daily records of rainfall R_{hD} (mm) and mean wind speed U_{10D} (m/s), the scalar "absolute spell index" (mm/absolute spell) can be approximated by calculating the airfield driving rain associated with

this absolute period, thereby eliminating the directional component and considering in the summation the data from those days contained within the absolute spell as follows:

$$I'_{AS} = \frac{2}{9}\sum U_{10D} \cdot \left(R_{hD}\right)^{8/9} \quad (7)$$

Considering the driving rain calculated for each of the absolute spells existing in a year by Eq. (7) (I'_{AS}), a historical series was developed for each location with the annual maximum values. This collection of maximum values allows for similar calculations of the driving rain expected for a return period of three years (I_{AS}) based on the Gumbel distribution, as in the example shown in Table 5. All these operations have been calculated using a macro in a spreadsheet program and analyzed for all weather stations. The results obtained are shown in Table 6.

Table 5. Calculation example of driving rain expected for a return period of 3 years I_{AS}.

Table 6. I_{AS} for 80 sites spread across the Spanish territory *(stations with daily records for 50 years are italicised).*

As the period considered is smaller, the index obtained by strictly applying the ISO standard is also lower. Using daily data and not hourly data also prevents the direct comparison of both I_S and I_{AS} results. Nevertheless, the proposed scalar index supplements the characterisation provided by the *daDRI*, estimating the exposure during particular stages of wetting.

In this way, locations where the short-term exposure is comparatively unfavourable are identified. Such circumstances should be characterised in the same way as the annual exposure, as two sites with similar

annual exposure may be subject to short-term conditions of wetting by very different amounts of driving rain, depending on the intensity with which this exposure is spread over time.

Although the higher specific values are found in locations with a high annual exposure (Santiago, San Sebastián, Tarifa, La Coruña), comparatively high specific exposures at locations with low annual exposure are also identified (the Balearic Islands, the Mediterranean coast and southwest of the peninsula).

4.2 Comparison of I_S and I_{AS}

This study has also used hourly data from seven stations, with the oldest hourly data provided by AEMET and representative of different levels of recorded annual exposure (the Madrid airport and the Barcelona airport are "sheltered", the Jerez airport and the Bilbao airport are "moderate", San Sebastián-Igueldo and the Vigo airport are "high" and the Santiago airport is "severe").

With these data, the I_S indices linked with spells according to ISO 15927-3:2009 have been obtained. Although these hourly data go back only 14 years (1998-2011), they allow for the estimation of the degree of convergence between I_{AS} and the index defined by the ISO standard.

The results obtained for the orientation of greatest exposure are shown with the index I_{AS} on the same sites. The scalar approximation of the exposure during stages of wetting has a reasonable degree of convergence with respect to the maximum directional index I_S, as shown in Figure 10. The good correlation coefficient suggests that the convergence identified could be extrapolated to other locations where there are no representative hourly records. Since the number of sites included in the analysis is small, more sites have to be studied for a sounder conclusion to be drawn.

Fig. 10. Convergence of $I_S - I_{AS}$ exposure results.

4.3 Multi-criteria characterisation of wetting exposure

Using the indices obtained to characterise the annual exposure and short-term exposure, a map of multi-criteria exposure, which integrates both indices, has been produced. For this reason, in addition to the levels defined by Lacy for the index *aDRI*, four different exposure levels (A to D) associated with the I_{AS} value obtained were set, as shown in Figure 11 ($0{,}72 \cdot I_{ASmax} <$ **A**; $0{,}36 \cdot I_{ASmax} <$ **B** $\leq 0{,}72 \cdot I_{ASmax}$; $0{,}18 \cdot I_{ASmax} <$ **C** $\leq 0{,}36 \cdot I_{ASmax}$; **D** $\leq 0{,}18 \cdot I_{ASmax}$). As a result, the annual exposure rate (*daDRI*) is represented, together with the estimated exposure level for the absolute spell (I_{AS}).

This analysis extends the information in the map drawn in Figure 2 by refining the annual exposure with the exposure relative to specific stages of wetting, characterising the short-term risk of water penetration.

Fig. 11. Wetting exposure multi-criteria map of Spain.

Overall, 35% of sites have a spell of absolute exposure that might be considered relevant ("A" - "B"), with a similar proportion to the number of locations characterised as "non-sheltered" against annual exposure.

The simultaneous analysis of the annual and instantaneous exposure in specific wetting stages is particularly important in locations in the northern part of the country, southwest of the peninsula and in certain parts of the Canary Islands, where the short-term exposure is more pronounced.

It is interesting to note that certain sites with very low annual exposure, such as those located on the Mediterranean coast (Barcelona, Murcia, Valencia, Palma), also have degrees of short-term exposure that are comparatively high compared to their annual exposure. In this study, the existence of typical seasonal heavy rainfall at these sites is identified [33].

Notwithstanding the above, overall, a high annual exposure typically results in more lasting and more intense wetting stages, resulting in that sites with higher annual exposure located on the north coast of the country (Santiago de Compostela, San Sebastián, Vigo) also consistently present more intense stages of wetting.

In response to both factors, the entire interior of the country, except for mountain stations, is subjected to both long and short-term exposure and largely protected from the action of driving rain and moisture.

5. Conclusions

This study presents important contributions to the knowledge of exposure to driving rain on vertical building façades in Spain.

Based on daily data from 80 weather stations located throughout the country, the severity of the annual exposure has been classified using the *aDRI* index. A map of driving rain in Spain was produced. With this work, Spain joins the countries that have developed zoning maps updated to estimate the exposure of driving rain, and the rates obtained for Spain were comparable to those of other countries.

Mathematical adjustments have been established that allow for the accurate estimation of the *daDRI* daily rate from monthly or annual average data in any location in Spain. It has been shown that these adjustments are very similar to those reported for Greece, another country with a Mediterranean climate.

The error derived from the use of monthly and annual climatic data has been analysed regarding daily results, and the different root causes of loss of precision in the estimate have been identified and weighed. The magnitude of the error of co-occurrence is roughly similar to that of the error of averaging the climate data according to the results obtained in the Spanish locations.

Finally, a new scalar indicator I_{AS} has been presented to estimate the severity of the exposure during specific stages of wetting, complementing the previous annual characterisation. To accomplish this task, a new absolute spell has been defined that can be calculated from daily weather data. This new index has proven to be convergent with the index I_S defined by ISO 15927-3:2009.

The representation of the index associated with absolute spells, in addition to the annual driving rain index map, allows for a more precise estimation of the exposure, simultaneously calculating the exposure on a yearly and short-term basis. A new map that includes both criteria has been produced for Spain.

The characterisation obtained complements and objectively enhances the estimation of the degree of exposure to moisture provided by the Spanish standard, providing an extremely useful tool for the subsequent association of different construction types of façades at different Spanish sites.

Acknowledgements

The results presented were obtained from information provided by the Spanish Meteorological Agency, Ministry of Environment, Rural and Marine Affairs (AEMET). We acknowledge the partial funding of the Research Project BIA2008-00058 (VI Spanish National Plan for Scientific Research, Technological Development and Innovation 2008-2011). We also recognise Javier Escuer Gracia for his help in preparing the maps.

References

[1] Tang W, Davidson CI, Finger S, Vance K. Erosion of limestone building surfaces caused by wind-driven rain. 1. Field measurements. Atmospheric Environment 2004; 38(33): 5589-99. (doi:10.1016/j.atmosenv.2004.06.030)

[2] Morrison Hershfield Limited. Survey of building envelope failures in the coastal climate of British Columbia. Canada Mortgage and Housing Corporation; 1996.

[3] Sanders C. Heat, air and moisture transfer in insulated envelope parts: Environmental conditions. International Energy Agency, Annex 24, Final report, vol. 2. Leuven: 1996.

[4] del Coz J.J, García P.J, Díaz Pérez L.M, Riesgo Fernández P. Nonlinear thermal analysis of multi-holed lightweight concrete blocks used in external and non-habitable floors by FEM. International Journal of Heat and Mass Transfer 2011; 54(1–3): 533-548

[5] del Coz J.J, García P.J, Súarez J.L, Rabanal F.P, Lozano A, Domínguez J. Non-linear heat analysis of the performance of light concrete hollow brick walls by FEM. In: J.W. Bull editor. Computer Analysis and design of masonry structures. Saxe-Coburg Publications; 2012.

[6] Spanish Ministry of Housing. Spanish Building Technical Code. Basic Document HS1, Resistance to moisture. Madrid; 2006.

[7] Hoppestad S. Slagregn i Norge (*Driving rain in Norway, in Norwegian*). Norwegian Building Research Institute Report no. 13, Oslo: NBI; 1955.

[8] Lacy RE. Driving-rain maps and the onslaught of rain on buildings. Proceedings of RILEM/CIB symposium on moisture problems in buildings, Helsinki: 1965.

[9] Blocken B, Carmeliet J. A review of wind-driven rain research in building science. J. Wind Eng. Ind. Aerodyn. 2004; 92(13): 1079–130. (doi:10.1016/j.jweia.2004.06.003)

[10] Blocken B, Carmeliet J. Overview of three state-of-the-art wind-driven rain assessment models and comparison based on model theory. Building and Environment 2010; 45(3):691-703. (doi:10.1016/j.buildenv.2009.08.007)

[11] Blocken B, Deszö G, van Beeck J, Carmeliet J. Comparison of calculation models for wind-driven rain deposition on building facades. Atmospheric Environment 2010; 44(14):1714-1725. (doi:10.1016/j.atmosenv.2010.02.011)

[12] Blocken B, Abuku M, Nore K, Briggen P.M, Schellen H.L, Thue J.V, Roels S, Carmeliet J. Intercomparison of wind-driven rain deposition models based on two case studies with full-scale measurements. J. Wind Eng. Ind. Aerodyn. 2011; 99(4): 448–459. (doi:10.1016/j.jweia.2010.11.004)

[13] Blocken B, Carmeliet J. Guidelines for the required time resolution of meteorological input data for wind-driven rain calculations on buildings. J. Wind Eng. Ind. Aerodyn. 2008; 96(5): 621–39. (doi:10.1016/j.jweia.2008.02.008)

[14] Blocken B, Carmeliet J. On the error associated with the use of hourly data in wind-driven rain calculations on building facades. Atmospheric Environment 2007; 41(11):2335-43. (doi:10.1016/j.atmosenv.2006.11.014)

[15] Lacy RE, Shellard HC. An index of driving rain. The Meteorological Magazine 1962; 91(1080):177-84.

[16] Grimm CT. A driving rain index for masonry walls. In: Borchelt JG, editor. Masonry: Materials, properties and performance. ASTM STP 778. P. 171-7.

[17] Boyd, DW. Driving rain map of Canada. Technical note no. 398. Ottawa: National Research Council Canada; 1963.

[18] Giarma C, Aravantinos D. Estimation of building components' exposure to moisture in Greece based on wind, rainfall and other climatic data. J. Wind Eng. Ind. Aerodyn. 2011; 99: 91-102. (doi:10.1016/j.jweia.2010.12.001)

[19] Sahal N. Proposed approach for defining climate regions for Turkey based on annual driving rain index and heating degree-days for building envelope design. Building and Environment 2006; 41: 520-6. (doi:10.1016/j.buildenv.2005.07.004)

[20] Sauer P. An annual driving rain index for China. Building and Environment 1987; 22:239-40. (doi:10.1016/0360-1323(87)90016-3)

[21] Chand I, Bhargava PK. Estimation of driving rain index for India. Building and Environment 2002; 37: 549-54. (doi:10.1016/S0360-1323(01)00057-9)

[22] Blocken B, Carmeliet J. On the validity of the cosine projection in wind-driven rain calculations on buildings. Building and Environment 2006; 41(9):1182-9. (doi:10.1016/j.buildenv.2005.05.002)

[23] EN ISO 15927-3:2009 Hygrothermal performance of buildings — Calculation and presentation of climatic 7data Part 3: Calculation of a driving rain index for vertical surfaces from hourly wind and rain data. European Committee for Standardization; 2009.

[24] Boyd DW. Weather and the deterioration of buildings materials. In: ASTM Special Technical Publication no. 691. Durability of Building Materials and Components. Ottawa: DBR-P-933; 1980, p. 145-56.

[25] Rydock JP, Gustavsen A. A look at driving rain spells at three cities in Great Britain. Building and Environment 2007; 42:1386-90. (doi:10.1016/j.buildenv.2005.11.020)

[26] Rydock JP, Lisø KR, Forland EJ, Nore K, Thue JV. A driving rain exposure index for Norway. Building and Environment 2005; 40:1450-8. (doi:10.1016/j.buildenv.2004.11.018)

[27] Avendano P. Present state of EXCO's research on rain penetration of buildings. CIB Working Commission on Rain Penetration, Madrid: 1966.

[28] Straube JF, Burnett EFP. Simplified Prediction of Driving Rain Deposition. In: Proc. of International Building Physics Conference, Eindhoven: 2000; p. 375-382.

[29] Spanish National Meteorological Agency. http://www.aemet.es/es/servidor-datos/acceso-datos/listado-contenidos/detalles/series_climatologicas. (Accessed 14 Feb. 2012)

[30] Kottek M, Grieser J, Beck C, Rudolf B, Rubel F. World Map of the Köppen-Geiger climate classification updated. Meteorol. Z. 2006; 15:259-63. (doi: 10.1127/0941-2948/2006/0130).

[31] Spanish Ministry of Public Works. Statistical information of Buildings. http://www.fomento.gob.es/mfom/lang_castellano/Estadisticas_y_Publicaciones/Informacion_Estadistica/Construccion/ConstruccionEdificios/Lmo_Publicacion/default.htm. (Accessed 14 Feb. 2012)

[32] Kvande T, Lisø KR. Climate adapted design of masonry structures. Building and Environment 2009; 44(12):2442-50. (doi:10.1016/j.buildenv.2009.04.007)

[33] Llasat MC, Martín F, Barrera A. From the concept of ‘‘Kaltlufttropfen’’ (cold air pool) to the cut-off low. The case of September 1971 in Spain as an example of their role in heavy rainfalls. Meteorol Atmos Phys 2007; 96: 43–60. (doi: 10.1007/s00703-006-0220-9)

List of tables

Table 1.

Determination of the degree of exposure to wind. Source: SBTC (DB-HS1).

WIND EXPOSURE DEGREE		Terrain roughness					
		Urban area			Others		
		Wind zone *(from map)*			**Wind zone** *(from map)*		
		A	**B**	**C**	**A**	**B**	**C**
Building height (m)	<15	V3	V3	V3	V2	V2	V2
	16-40	V3	V2	V2	V2	V2	V1
	41-100	V2	V2	V2	V1	V1	V1

Table 2.

Determination of the degree of exposure to moisture. Source: SBTC (DB-HS1).

MOISTURE EXPOSURE DEGREE		**Mean annual rainfall zone** *(from map)*				
		I	**II**	**III**	**IV**	**V**
Wind exposure degree	V1	5	5	4	3	2
	V2	5	4	3	3	2
	V3	5	4	3	2	1

Table 3.

Driving rain indices for 80 sites spread across the Spanish territory *(stations with daily records for 50 years are italicised).*

LOCATION	ALT. [m]	LATITUDE (DMS)	LONGITUDE (DMS)	daDRI [m^2/s]	maDRI [m^2/s]	aaDRI [m^2/s]
La Coruña airport	98	43º18'25"N	08º22'20"W	5,52	4,38	4,13
La Coruña	58	43º22'02"N	08º25'10"W	4,70	3,83	3,61
Santiago airport	370	42º53'16"N	08º24'39"W	11,05	7,84	7,19
Vitoria airport	513	42º52'55"N	02º44'06"W	2,38	2,04	2,02
Albacete (Los Llanos)	704	38º57'08"N	01º51'47"W	1,66	1,60	1,60
Alicante airport	43	38º16'58"N	00º34'15"W	1,12	1,04	1,06
Alicante	81	38º22'21"N	00º29'39"W	0,81	0,77	0,79
Almería airport	21	36º50'47"N	02º21'25"W	0,99	0,92	0,92
Asturias airport	127	43º34'01"N	06º02'39"W	4,67	3,73	3,59
Oviedo	336	43º21'16"N	05º52'22"W	3,37	2,82	2,72
Ávila	1130	40º39'33"N	04º40'48"W	1,28	1,13	1,10
Badajoz airport	185	38º53'00"N	06º49'45"W	1,95	1,51	1,44
Barcelona airport	4	41º17'34"N	02º04'12"E	2,66	2,38	2,38
Burgos (Villafría)	890	42º21'22"N	03º37'57"W	3,07	2,52	2,42
Cáceres	405	39º28'20"N	06º20'22"W	2,49	1,78	1,6
Cádiz	1	36º30'04"N	06º15'24"W	3,13	2,18	2,14
Jerez airport	27	36º45'02"N	06º03'21"W	3,74	2,47	2,39
Tarifa	32	36º00'55"N	05º35'51"W	5,82	5,42	5,60
Santander airport	5	43º25'45"N	03º49'53"W	6,50	5,06	4,89
Santander	52	43º29'30"N	03º47'59"W	5,79	4,44	4,20
Castellón de la Plana	35	39º57'00"N	00º04'17"W	1,31	1,14	1,16
Ciudad Real	628	38º59'22"N	03º55'11"W	1,22	1,01	0,98
Córdoba airport	90	37º50'39"N	04º50'46"W	2,44	1,77	1,7
Cuenca	945	40º04'00"N	02º08'17"W	1,34	1,10	1,07
Gerona airport	143	41º54'42"N	02º45'48"E	2,05	1,87	1,86
Granada airport	567	37º11'23"N	03º47'22"W	0,91	0,77	0,83
Granada air base	687	37º08'13"N	03º37'53"W	1,16	0,90	0,97
Molina de Aragón	1056	40º50'40"N	01º53'07"W	1,38	1,16	1,13
San Sebastián airport	4	43º21'25"N	01º47'32"W	6,17	4,69	4,49
San Sebastián (Igueldo)	251	43º18'27"N	02º02'22"W	9,46	7,28	6,86
Huelva	19	37º16'48"N	06º54'35"W	2,15	1,59	1,67
Huesca airport	541	42º05'00"N	00º19'35"W	2,16	2,09	2,12
Ibiza airport	6	38º52'35"N	01º23'04"E	1,92	1,61	1,62
Menorca airport	91	39º51'17"N	04º12'56"E	2,87	2,53	2,51
Palma de Mallorca airport	8	39º33'39"N	02º44'12"E	1,61	1,44	1,51
Palma de Mallorca port	3	39º33'12"N	02º37'31"E	1,02	0,86	0,87
Jaén	582	37º46'40"N	03º48'27"W	1,52	1,02	0,95
Logroño airport	353	42º27'08"N	02º19'52"W	1,41	1,37	1,37
Fuerteventura airport	25	28º26'41"N	13º51'47"W	0,60	0,58	0,63
Lanzarote airport	14	28º57'07"N	13º36'01"W	0,66	0,6	0,69
Las Palmas de G. C. airport	24	27º55'21"N	15º23'22"W	0,71	0,73	0,93
León airport	916	42º35'20"N	05º38'58"W	1,76	1,60	1,57
Ponferrada	534	42º33'50"N	06º36'00"W	1,28	1,14	1,16
Lérida	192	41º37'33"N	00º35'42"E	0,80	0,82	0,82
Madrid airport	609	40º28'00"N	03º33'20"W	1,36	1,17	1,13
Madrid (Cuatro Vientos)	687	40º22'40"N	03º47'21"W	1,62	1,31	1,26
Madrid (Getafe)	617	40º18'00"N	03º43'21"W	1,62	1,32	1,28
Madrid	667	40º24'43"N	03º40'41"W	1,18	1,03	1,01
Madrid (Torrejón)	611	40º29'00"N	03º27'01"W	1,21	1,04	1,03
Navacerrada mountain pass	1894	40º46'50"N	04º00'37"W	7,07	4,77	4,26
Málaga airport	7	36º40'00"N	04º29'17"W	1,98	2,14	2,19
Melilla	47	35º16'40"N	02º57'19"W	1,80	1,54	1,53
Murcia (Alcantarilla)	85	37º57'28"N	01º13'47"W	0,69	0,67	0,72
San Javier airport	4	37º47'20"N	00º48'12"W	1,79	1,36	1,34
Pamplona airport	459	42º46'37"N	01º39'00"W	2,42	2,32	2,39
Pontevedra	108	42º26'24"N	08º36'59"W	4,36	3,40	3,31
Vigo airport	261	42º14'22"N	08º37'26"W	8,21	6,36	6,19
Salamanca airport	790	40º57'34"N	05º29'54"W	1,78	1,38	1,28
Salamanca	775	40º57'23"N	05º39'41"W	1,29	0,93	0,87
Segovia	1005	40º56'52"N	04º07'38"W	1,35	1,11	1,06

Morón de la Frontera	87	37º09’30”N	05º36’57”W	3,18	2,10	1,99
Sevilla airport	34	37º25’00”N	05º52’45”W	2,65	1,87	1,78
Soria	1082	41º46’30”N	02º28’59”W	1,78	1,59	1,55
Hierro airport	32	27º49’08”N	17º53’20”W	1,05	1,03	1,14
Izaña	2371	28º18’32”N	16º29’58”W	6,10	3,52	3,02
La Palma airport	33	28º37’59”N	17º45’18”W	2,14	1,65	1,76
Sta. Cruz de Tenerife	35	28º27’48”N	16º15’19”W	0,78	0,65	0,65
North Tenerife airport	632	28º28’39”N	16º19’46”W	3,61	2,75	2,94
South Tenerife airport	64	28º02’51”N	16º33’39”W	0,72	0,75	0,79
Reus airport	71	41º08’59”N	01º10’44”E	1,70	1,77	1,84
Tortosa	44	40º49’14”N	00º29’29”E	1,33	1,59	1,70
Toledo	515	39º53’05”N	04º02’58”W	1,09	0,94	0,91
Valencia airport	69	39º29’12”N	00º28’24”W	1,66	1,63	1,70
Valencia	11	39º28’50”N	00º21’59”W	1,11	0,93	0,96
Valladolid (Villanubla)	846	41º42’00”N	04º51’00”W	2,30	1,83	1,73
Valladolid	735	41º39’00”N	04º46’00”W	1,18	1,10	1,07
Bilbao airport	42	43º17’53”N	02º54’21”W	5,10	4,16	4,01
Zamora	656	41º31’00”N	05º44’01”W	1,17	0,97	0,94
Daroca	779	41º06’53”N	01º24’39”W	0,69	0,73	0,73
Zaragoza airport	247	41º39’43”N	01º00’29”W	1,23	1,49	1,54

Table 4.

Summary of the errors derived from the non co-occurrence of wind and rain (e_1) and from the averaged data (e_2) at 78 Spanish sites.

LOCATION	maDRI			aaDRI		
	e_1 [%]	e_2 [%]	$e_1 + e_2$ [%]	e_1 [%]	e_2 [%]	$e_1 + e_2$ [%]
La Coruña airport	-8,86	-11,81	-20,67	-10,20	-15,02	-25,22
La Coruña	-9,51	-9,09	-18,60	-10,29	-12,83	-23,12
Santiago airport	-7,76	-21,30	-29,06	-8,25	-26,67	-34,92
Vitoria airport	-7,75	-6,51	-14,26	-8,47	-6,79	-15,26
Albacete (Los Llanos)	-10,94	7,47	-3,47	-15,26	11,53	-3,72
Alicante airport	-4,03	-2,59	-6,62	-2,73	-2,58	-5,31
Alicante	-3,69	-1,33	-5,02	-2,79	-0,07	-2,86
Almería airport	-8,39	1,21	-7,18	-6,78	-0,48	-7,26
Asturias airport	-6,79	-13,40	-20,19	-7,24	-16,01	-23,25
Oviedo	-5,70	-10,40	-16,11	-6,49	-12,63	-19,12
Ávila	-9,58	-2,09	-11,67	-14,13	-0,08	-14,21
Badajoz airport	-16,00	-6,50	-22,50	-19,43	-6,70	-26,13
Barcelona airport	-1,16	-9,35	-10,50	-0,78	-9,67	-10,45
Burgos (Villafría)	-9,71	-8,33	-18,04	-12,65	-8,55	-21,21
Cáceres	-0,41	-28,37	-28,78	-5,77	-29,89	-35,66
Cádiz	-15,33	-14,98	-30,30	-14,69	-16,99	-31,68
Jerez airport	-19,30	-14,70	-34,00	-18,45	-17,81	-36,26
Tarifa	-4,32	-2,58	-6,91	-0,80	-3,06	-3,86
Santander airport	-9,15	-12,90	-22,06	-9,44	-15,35	-24,80
Santander	-0,06	-23,26	-23,32	-0,11	-27,39	-27,50
Castellón de la Plana	-0,91	-11,61	-12,52	0,88	-12,22	-11,34
Ciudad Real	-15,43	-1,32	-16,75	-17,64	-1,65	-19,29
Córdoba airport	-0,29	-27,33	-27,62	-2,47	-27,82	-30,28
Cuenca	-12,17	-5,81	-17,98	-14,15	-6,19	-20,34
Gerona airport	-3,13	-5,96	-9,09	-2,99	-6,56	-9,55
Granada airport	-12,05	-3,52	-15,57	-6,04	-3,18	-9,21
Granada air base	-12,46	-10,32	-22,78	-5,70	-10,57	-16,28
Molina de Aragón	-13,68	-1,76	-15,45	-20,67	2,60	-18,07
San Sebastián airport	-10,17	-13,72	-23,88	-11,06	-16,22	-27,28
San Sebastián (Igueldo)	-9,24	-13,76	-23,00	-10,70	-16,74	-27,45
Huelva	-15,47	-10,86	-26,33	-11,30	-11,25	-22,55
Huesca airport	2,22	-5,42	-3,20	3,02	-5,03	-2,00
Ibiza airport	-9,21	-6,92	-16,13	-10,41	-5,18	-15,59
Menorca airport	-8,31	-3,56	-11,87	-9,70	-2,84	-12,54
Palma de Mallorca airport	-7,90	-2,78	-10,68	-6,63	0,03	-6,61
Palma de Mallorca port	-10,59	-4,90	-15,49	-10,48	-3,85	-14,33
Jaén	-0,51	-32,16	-32,68	-5,15	-32,30	-37,45
Logroño airport	-7,09	3,84	-3,25	-10,04	6,77	-3,28
Fuerteventura airport	-1,47	-2,59	-4,07	3,98	-0,35	3,63
Lanzarote airport	-6,05	-2,60	-8,66	6,65	-1,86	4,79
Las Palmas de G. C. airport	-6,87	8,47	1,60	12,13	17,77	29,90
León airport	-12,04	2,53	-9,51	-17,23	5,92	-11,31
Ponferrada	-13,07	1,68	-11,39	-14,05	4,24	-9,81
Lérida	7,25	-4,62	2,64	12,87	-10,20	2,67
Madrid airport	-15,09	0,76	-14,32	-18,59	1,56	-17,03
Madrid (Cuatro Vientos)	-15,62	-3,22	-18,84	-19,25	-2,76	-22,02
Madrid (Getafe)	-17,68	-1,07	-18,75	-20,74	-0,36	-21,09
Madrid	-11,67	-0,45	-12,11	-15,20	0,90	-14,30
Madrid (Torrejón)	-11,58	-2,23	-13,81	-14,18	-1,22	-15,40
Málaga airport	12,71	-4,63	8,09	14,27	-3,62	10,66
Melilla	-8,28	-6,31	-14,59	-5,89	-9,21	-15,10
Murcia (Alcantarilla)	1,65	-4,64	-2,99	8,20	-4,73	3,48
San Javier airport	-12,52	-11,78	-24,29	-8,83	-16,06	-24,89
Pamplona airport	-3,62	-0,30	-3,93	-2,60	1,60	-1,00
Pontevedra	-0,14	-21,84	-21,98	-0,16	-23,89	-24,05
Vigo airport	-6,36	-16,15	-22,51	-5,01	-19,63	-24,64
Salamanca airport	-0,47	-21,85	-22,32	-1,83	-26,13	-27,95
Salamanca	-0,58	-27,26	-27,84	-1,32	-31,31	-32,64

Segovia	-14,84	-3,45	-18,29	-19,00	-2,38	-21,37
Morón de la Frontera	-20,87	-12,98	-33,85	-21,37	-16,12	-37,48
Sevilla airport	-17,43	-13,01	-30,44	-16,99	-16,01	-32,99
Soria	-9,40	-1,29	-10,69	-13,87	0,71	-13,17
Hierro airport	0,72	-2,47	-1,75	10,46	-1,62	8,84
La Palma airport	-10,73	-11,91	-22,64	-5,71	-11,99	-17,69
Sta. Cruz de Tenerife	-11,30	-5,25	-16,55	-10,17	-6,79	-16,96
North Tenerife airport	-13,47	-10,29	-23,76	-10,74	-8,03	-18,77
South Tenerife airport	1,10	2,85	3,95	8,62	1,20	9,82
Reus airport	8,89	-4,41	4,47	10,82	-2,47	8,34
Tortosa	15,79	4,27	20,05	19,39	8,25	27,64
Toledo	-12,61	-1,73	-14,34	-15,52	-1,12	-16,64
Valencia airport	2,72	-4,28	-1,57	3,65	-1,14	2,51
Valencia	-3,05	-13,36	-16,42	-0,67	-13,06	-13,73
Valladolid (Villanubla)	-15,07	-5,60	-20,67	-20,28	-4,44	-24,72
Valladolid	-9,84	3,42	-6,42	-13,29	4,18	-9,11
Bilbao airport	-7,43	-10,91	-18,34	-8,12	-13,15	-21,27
Zamora	-12,69	-4,49	-17,17	-16,44	-3,67	-20,11
Daroca	-2,97	8,62	5,65	-8,83	14,37	5,54
Zaragoza airport	14,36	7,57	21,93	14,18	11,52	25,70
AVERAGE RESULTS	**-6,98**	**-6,99**	**-13,97**	**-6,75**	**-7,06**	**-13,81**

Table 5.

Calculation example of driving rain expected for a return period of 3 years I_{AS}.

Santiago airport. Station 1428. 42º53'16"N 08º24'39"W			
Year	Maximum value of yearly I'$_{AS}$ (mm/absolute spell)	Year	Maximum value of yearly I'$_{AS}$ (mm/absolute spell)
1962	1069,87	1987	916,57
1963	1385,52	1988	676,20
1964	594,99	1989	737,81
1965	361,90	1990	378,84
1966	2339,14	1991	471,57
1967	577,99	1992	428,83
1968	450,66	1993	528,32
1969	477,18	1994	583,82
1970	771,33	1995	584,46
1971	539,41	1996	628,76
1972	937,45	1997	401,24
1973	319,98	1998	443,48
1974	647,88	1999	285,58
1975	465,12	2000	338,12
1976	613,10	2001	1554,31
1977	1175,57	2002	647,77
1978	776,22	2003	486,72
1979	780,55	2004	356,46
1980	356,61	2005	496,18
1981	292,80	2006	593,93
1982	749,51	2007	363,86
1983	453,98	2008	243,12
1984	363,56	2009	406,32
1985	361,71	2010	300,79
1986	859,29	2011	206,73

Magnitude	Value	Comment
N	50	Number of x_I data.
$\bar{x}$	615,622	Data average: $\bar{x} = \sum x_i / N$
σ_x	370,981	Standard deviation: $\sigma_x = \sqrt{\sum (x_i - \bar{x})^2 / N}$
u_y	0,548	Data average of 1 to N y_i values (reduced variable): $y_i = -\ln(\ln(N+1/i))$ *(Only depends on N value and could be approximated by a constant value of 0,5772)*
σ_y	1,161	Standard deviation of 1 to N y_i values (reduced variable): $y_i = -\ln(\ln(N+1/i))$ *(Only depends on N value and could be approximated by a constant value of 1,2856)*
u	440,292	Mode: $u = \bar{x} - u_y \frac{\sigma_x}{\sigma_y}$
α	0,003129	Dispersion parameter: $\alpha = \frac{\sigma_y}{\sigma_x} = \frac{1}{\beta}$

Cumulative distribution function. $F(x;\alpha;u) = \exp^{-\exp^{-y}} = \exp^{-\exp^{-\alpha(x-u)}}$

Return period	3 years	Taken in similarity to the I_S parameter of ISO standard
1 – F(x;u;α)	0,3333	Probability of exceeding the x value.
x value	**728,828**	I_{AS} value (maximum I'_{AS} likely to occur once every 3 years in mm/absolute spell).

Table 6.

I_{AS} for 80 sites spread across the Spanish territory *(stations with daily records for 50 years are italicised).*

LOCATION	I_{AS} [mm/absolute spell]	LOCATION	I_{AS} [mm/absolute spell]
La Coruña airport	364,71	*Las Palmas de G. C. airport*	63,97
La Coruña	296,14	*León airport*	100,26
Santiago airport	728,83	Ponferrada	78,13
Vitoria airport	127,82	*Lérida*	36,20
Albacete (Los Llanos)	75,88	*Madrid airport*	74,65
Alicante airport	62,65	*Madrid (Cuatro Vientos)*	87,73
Alicante	44,78	*Madrid (Getafe)*	85,91
Almería airport	59,62	Madrid	66,29
Asturias airport	274,18	Madrid (Torrejón)	64,82
Oviedo	185,93	*Navacerrada mountain pass*	459,94
Ávila	77,65	Málaga airport	133,99
Badajoz airport	118,33	Melilla	108,35
Barcelona airport	132,00	*Murcia (Alcantarilla)*	39,95
Burgos (Villafría)	182,13	*San Javier airport*	109,86
Cáceres	166,30	Pamplona airport	117,26
Cádiz	228,35	Pontevedra	286,68
Jerez airport	241,47	*Vigo airport*	503,81
Tarifa	396,08	*Salamanca airport*	99,71
Santander airport	344,05	Salamanca	78,81
Santander	316,13	Segovia	72,80
Castellón de la Plana	77,41	*Morón de la frontera*	203,11
Ciudad Real	70,86	*Sevilla airport*	179,42
Córdoba airport	168,75	*Soria*	94,21
Cuenca	67,36	Hierro airport	98,87
Girona airport	87,67	Izaña	608,23
Granada airport	56,08	La Palma airport	176,99
Granada air base	67,50	*Sta. Cruz de Tenerife*	62,69
Molina de Aragón	63,15	North Tenerife airport	206,18
San Sebastián airport	308,80	South Tenerife airport	66,12
San Sebastián (Igueldo)	475,94	*Reus airport*	81,12
Huelva	135,86	*Tortosa*	65,40
Huesca airport	88,15	*Toledo*	58,97
Ibiza airport	89,68	Valencia airport	96,62
Menorca airport	142,41	Valencia	71,49
Palma de Mallorca airport	80,06	Valladolid (Villanubla)	128,84
Palma de Mallorca port	49,95	Valladolid	68,26
Jaén	102,10	*Bilbao airport*	271,20
Logroño airport	59,72	Zamora	69,97
Fuerteventura airport	57,48	*Daroca*	27,44
Lanzarote airport	61,71	*Zaragoza airport*	52,83

Figure captions

Fig. 1. Map of wind zones (A, B, C) for wind gusts of 10 minutes and a 50-year return period (left) and the map of average annual rainfall zones (right) used by the Spanish standard. Source: SBTC (DB-HS1).

Fig. 2. Annual Driving Rain Index Map of Spain.

Fig. 3. Best-fit linear relationship between daDRI and maDRI.

Fig. 4. Best-fit linear relationship between daDRI and aaDRI.

Fig. 5. Best-fit linear relationship between maDRI and aaDRI.

Fig. 6. Comparison with Greek and Indian maDRI-aaDRI adjustments.

Fig. 7. Exposure indices calculated from the monthly average data according to both hypotheses in non-sheltered annual exposure stations. (e_1) The magnitude of the error derived from the non-co-occurrence of wind and rain. (e_2) The magnitude of the error derived from the averaged data.

Fig. 8. Exposure indices calculated from the annual average data according to both hypotheses in non-sheltered annual exposure stations. (e_1) The magnitude of the error derived from the non-co-occurrence of wind and rain. (e_2) The magnitude of the error derived from the averaged data.

Fig. 9. Definition of "*ISO spell*" and proposed "*absolute spell*".

Fig. 10. Convergence of I_S – I_{AS} exposure results.

Fig. 11. Wetting exposure multi-criteria map of Spain.

Figure 1

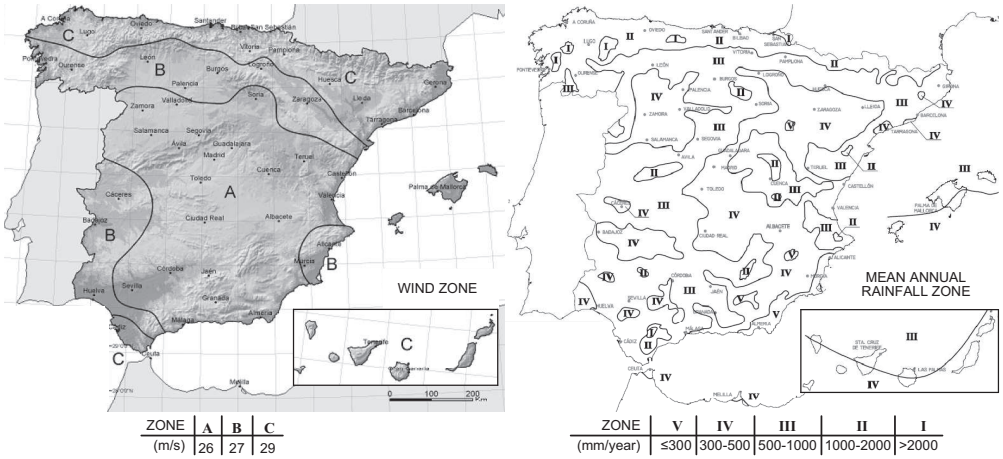

Fig. 1. Map of wind zones (A, B, C) for wind gusts of 10 minutes and a 50-year return period (left) and the map of average annual rainfall zones (right) used by the Spanish standard. Source: SBTC (DB-HS1).

Figure 2

Fig. 2. Annual Driving Rain Index Map of Spain.

Figure 3

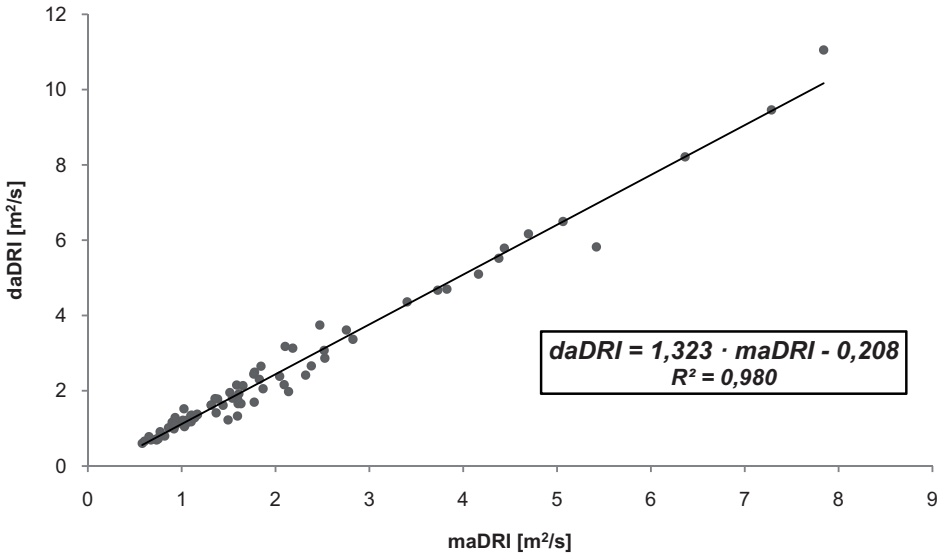

Fig. 3. Best-fit linear relationship between daDRI and maDRI.

Figure 4

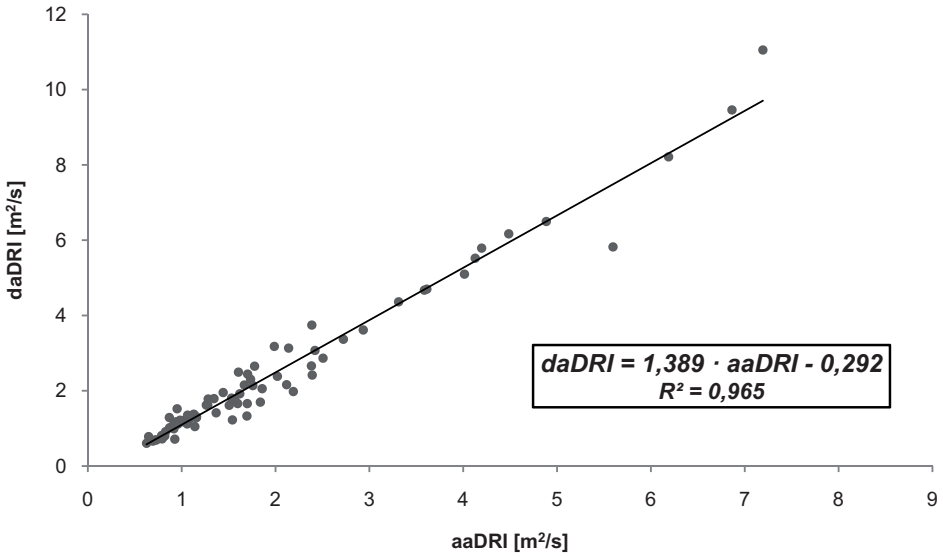

Fig. 4. Best-fit linear relationship between daDRI and aaDRI.

Figure 5

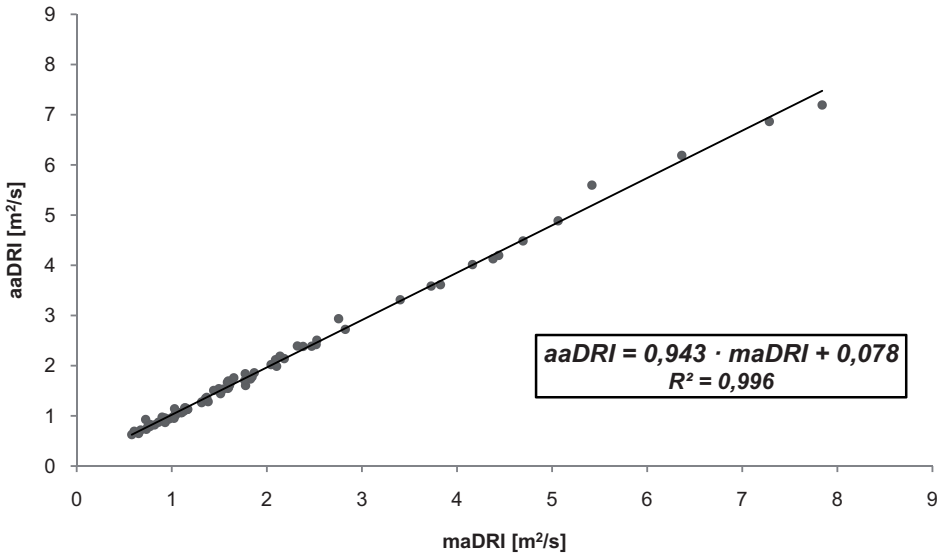

Fig. 5. Best-fit linear relationship between maDRI and aaDRI.

Figure 6 (changed brackets)

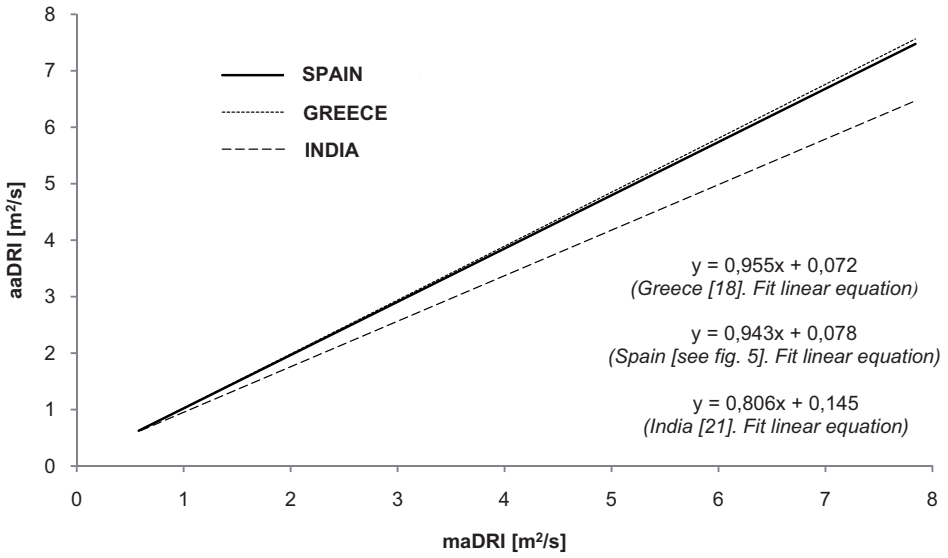

Fig. 6. Comparison with Greek and Indian maDRI-aaDRI adjustments.

Figure 7

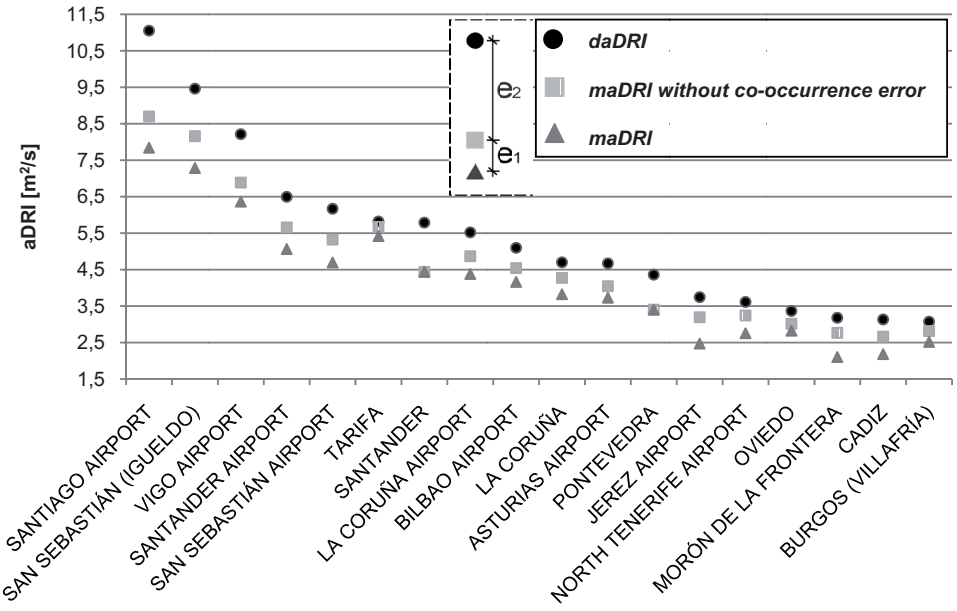

Fig. 7. Exposure indices calculated from the monthly average data according to both hypotheses in non-sheltered annual exposure stations. (*e1*) The magnitude of the error derived from the non-co-occurrence of wind and rain. (*e2*) The magnitude of the error derived from the averaged data.

Figure 8

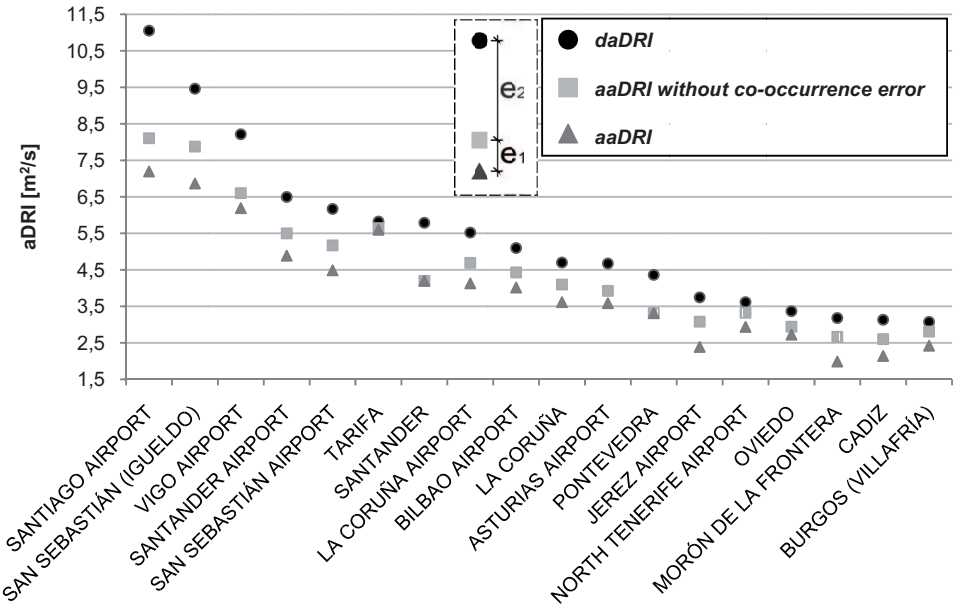

Fig. 8. Exposure indices calculated from the annual average data according to both hypotheses in non-sheltered annual exposure stations. (*e1*) The magnitude of the error derived from the non-co-occurrence of wind and rain. (*e2*) The magnitude of the error derived from the averaged data.

Figure 9

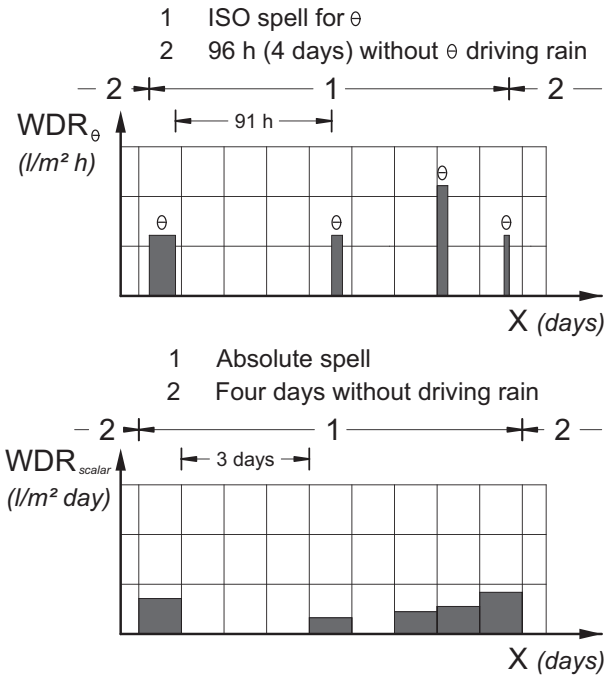

Fig. 9. Definition of “ISO spell” and proposed “absolute spell”.

Figure 10

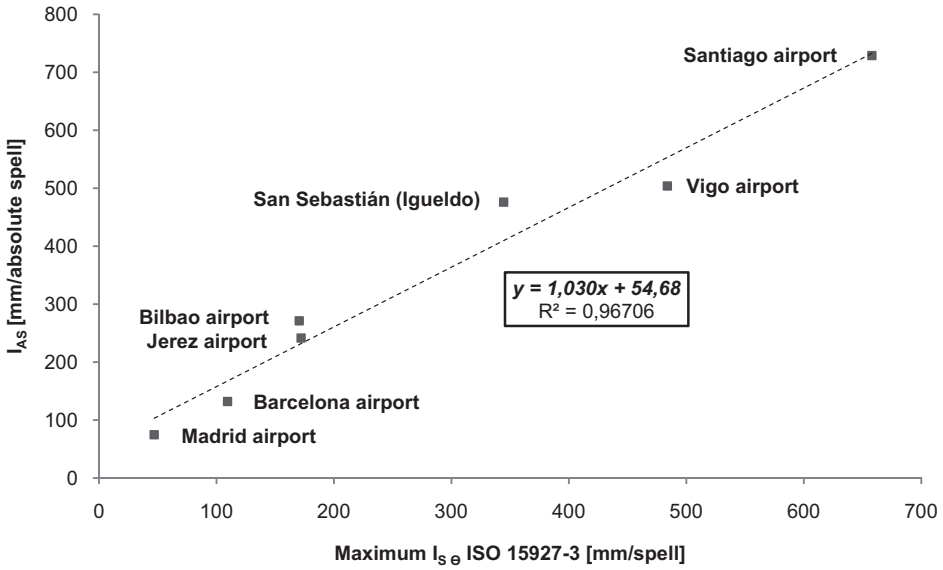

Fig. 10. Convergence of I_S – I_{AS} exposure results.

Figure 11

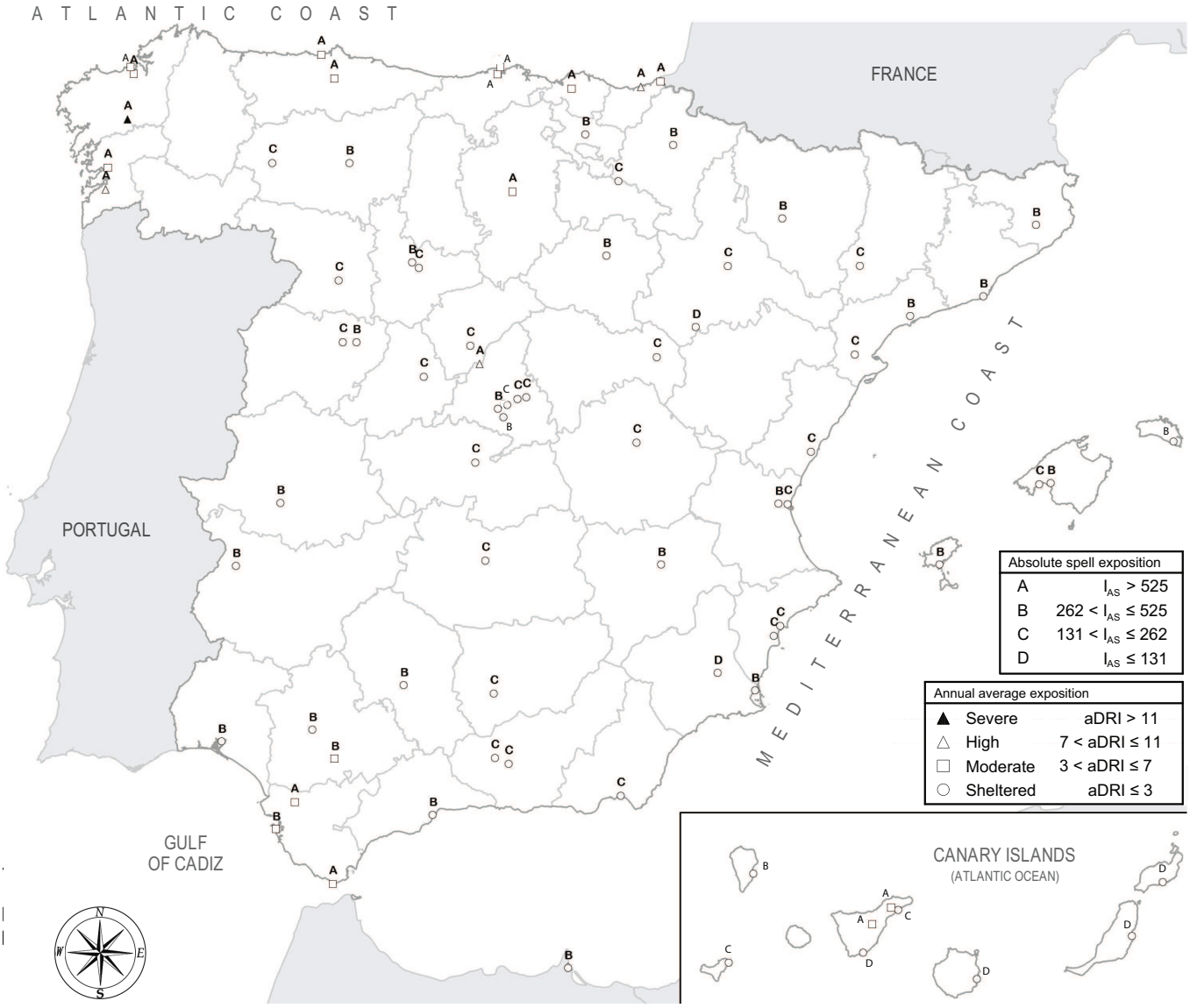

Fig. 11. Wetting exposure multi-criteria map of Spain.